A paramagnetic chemical exchange-based MRI probe metabolized by cathepsin D: design, synthesis and cellular uptake studies†

Mojmír Suchý,[a,b] Robert Ta,[b] Alex X. Li,[b] Filip Wojciechowski,[a] Stephen H. Pasternak,[c] Robert Bartha[b] and Robert H. E. Hudson*[a]

Received 22nd December 2009, Accepted 9th March 2010
First published as an Advance Article on the web 26th March 2010
DOI: 10.1039/b926639a

Overexpression of the aspartyl protease cathepsin D is associated with certain cancers and Alzheimer's disease; thus, it is a potentially useful imaging biomarker for disease. A dual fluorescence/MRI probe for the potential detection of localized cathepsin D activity has been synthesized. The probe design includes both MRI and optical reporter groups connected to a cell penetrating peptide by a cathepsin D cleavable sequence. This design results in the selective intracellular deposition (determined fluorimetrically) of the MRI and optical reporter groups in the presence of overexpressed cathepsin D. The probe also provided clearly detectable *in vitro* MRI contrast by the mechanism of paramagnetic chemical exchange effects (OPARACHEE).

Introduction

Cathepsin D is a member of the mammalian lysosomal aspartyl protease family found in all cells. However, cathepsin D (Cat D) is overexpressed in some cancers and in Alzheimer's disease (AD), which makes it a potentially useful marker for these diseases. Specifically, Cat D is upregulated in breast cancer,[1] ovarian cancer,[2] endometrial cancer[3] and prostate cancer,[4] and has been associated with an increased risk of metastasis.[5] Cat D may be involved in processes of early tumour progression including the stimulation of cell proliferation, fibroblast outgrowth and angiogenesis.[6,7] Therefore overexpression of this protease may have prognostic value[8] and help to identify subjects that require more aggressive treatment, making it an excellent target as an imaging biomarker. With respect to Alzheimer's disease (AD), a prevalent neurodegenerative brain disorder, it has been well documented that increased levels of lysosomal hydrolases in normal appearing neurons precede the earliest known histopathological features of AD.[9] Overexpression (up to 4 fold) of Cat D,[10–13] in Alzheimer's disease patients also makes this protease a viable imaging biomarker for nascent AD detection since very early clinical diagnosis remains difficult.[14]

A new method of generating contrast in magnetic resonance imaging (MRI) has been recently introduced based on chemical exchange saturation transfer (CEST).[15] Subsequently a large number of paramagnetic ion-containing lanthanide(III) complexes (containing metals other than gadolinium) have been found capable of inducing large hyperfine shifts of coordinated water protons as well as other exchangeable protons present in close proximity to the metal center.[16] These new MRI contrast agents are referred to as PARACEST MRI CAs.[17] Among other applications PARACEST MRI CAs have been successfully applied towards the detection of enzymatic activities; for example β-galactosidase,[18] caspase-3,[19] or urokinase plasminogen activator.[20] The PARACEST phenomenon exploits slowly exchanging water or protons in the ligand framework whereas agents with faster exchange rates can be used to generate contrast using on-resonance effects.

Within the framework of our interest in the development of MRI contrast agents capable of detecting important physiological parameters[21–24] we have designed and synthesized a probe for the MRI detection of localized Cat D enzymatic activity. The design adopts features of Tsien's earlier work which exploited a cell penetrating peptide (CPP) conjugated to a cleavable peptide domain and imaging agent cargo.[25] Probe **1** possesses four important structural features including a DOTA-like metal chelator, an optical tag for detection by fluorescent microscopy (to facilitate *in cultureo* cellular uptake studies), and a 23 amino acid containing peptide sequence possessing the TAT CPP sequence[26] and a protease-cleavable site (**1**, Fig. 1). A variety of passenger cargos have been shown to be transported intracellularly by TAT or other cell-penetrating peptides, such DNA, polymers, nanoparticles, liposomes, and small molecule based drugs and imaging agents.[26] The protease-cleavable site is expected to give selectivity for Cat D as it was designed on literature precedent and examination of the MEROPS peptidase database.[27]

The western half of probe **1** is designed to provide magnetic resonance imaging (MRI) contrast. The DOTA-like cage has been introduced in order to chelate Tm^{3+} (thulium ion), which will produce contrast using the mechanism of paramagnetic chemical exchange effects.[16a,28] The Tm^{3+} cation effectively produces contrast using the on-resonance paramagnetic chemical exchange effect (OPARACHEE),[29] which requires less radiofrequency energy

[a]*Department of Chemistry, The University of Western Ontario, London, Ontario, Canada, N6A 5B7. E-mail: robert.hudson@uwo.ca; Fax: 1 519-661-3022; Tel: 1 519-661-2111 ext. 86349*
[b]*Department of Medical Biophysics and the Imaging Research Group, Robarts Research Institute, 100 Perth Drive, The University of Western Ontario, London, Ontario, Canada, N6A 5K8*
[c]*Department of Physiology and Pharmacology, and the Molecular Brain Research Group, Robarts Research Institute, 100 Perth Drive, The University of Western Ontario, London, Ontario, Canada, N6A 5K8*

† Electronic supplementary information (ESI) available: High resolution mass spectral data for **1**, $\mathbf{1}_{cleaved}$ and data for the metabolism of **1** by Cat D. See DOI: 10.1039/b926639a

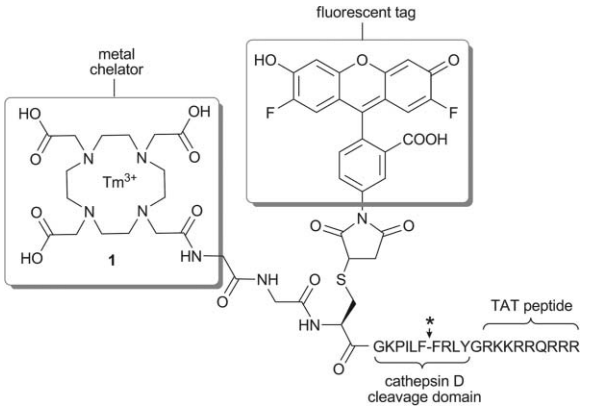

Fig. 1 Structure of probe **1** incorporating the fluorescent tag derived from Oregon Green® maleimide. The dominant Cat D cleavage site between phenylalanine (F) residues is indicated by an arrowhead with asterisk. Tm = thulium.

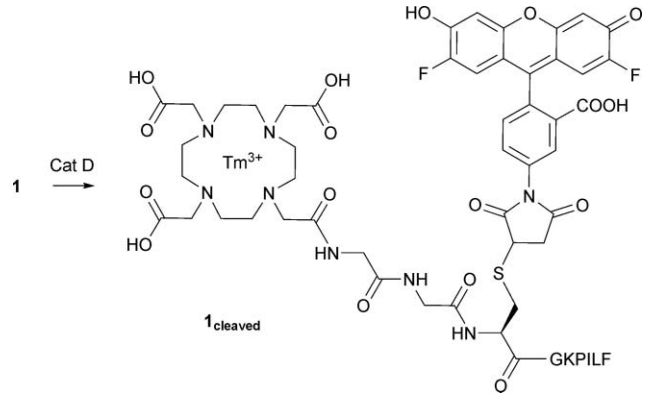

Scheme 1 The cathepsin D digestion of probe **1** initially gives the fragment $\mathbf{1}_{cleaved}$ which possesses the MR-active group and the Oregon Green® fluorophore.

than off-resonance PARACEST detection and therefore may be advantageous for *in vivo* imaging. Since the chemical exchange between bulk and bound water associated with the Tm^{3+} compounds is fast, the *Z*-spectrum of such compounds do not typically show a peak at the chemical shift of the exchangeable pool. Therefore, off-resonance excitation of the bound pool would be ineffective at the low power levels mandated by *in vivo* imaging applications. It is also possible to envision this moiety metalated with other lanthanide(III) cations (*e.g.* Gd^{3+}) in order to generate contrast by other effects.

The optical reporter was introduced for visualization of cellular uptake in cell culture or for future histological post mortem animal studies. It was attached to the cysteine primary sulfanyl group *via* a Michael addition to the commercially available maleimide dye—Oregon Green.[30] The bifunctional peptide sequence possesses a CPP to facilitate the potential transport of probe **1** across the blood brain barrier and promote cellular uptake, while the central portion of the peptide sequence (G to L) is a cleavage domain designed to be recognized by Cat D.[31]

As reported in the literature,[31,32] the Cat D-promoted enzymatic hydrolysis of peptides takes place between two lipophilic amino acid units, wherein two phenylalanine units were shown to be a superior substrate. In addition to the fluorophore-labelled MRI probe **1**, we have also prepared the expected major product of the Cat D-promoted enzymatic hydrolysis of **1** ($\mathbf{1}_{cleaved}$, Scheme 1). Fragment $\mathbf{1}_{cleaved}$ is expected to be formed upon the cleavage of the dual probe **1** within an intracellular compartment and represents the moiety that would be the origin of MRI contrast.

Probe **1** and the enzymatic hydrolysis product $\mathbf{1}_{cleaved}$ were synthesized and it was experimentally determined that probe **1** was metabolized by Cat D as predicted (see ESI†). Cellular uptake studies by fluorescence microscopy revealed selective accumulation of the probe within cells overexpressing Cat D and minimal accumulation in native cells. Furthermore, the expected probe metabolism product $\mathbf{1}_{cleaved}$ was detected *in vitro* by MRI using the OPARACHEE contrast mechanism. Together, these results provide the foundation for studies directed toward the localized detection of cathepsin D activity *in vivo*.

Results and discussion

Synthesis of DO3A terminal monomer

Monoalkylation[33] of DO3A *tert*-butyl ester (**2**) with *N*-bromoacetyl Gly-OBn (**3**)[34] followed by reductive removal (H_2, Pd/C, in EtOAc) of the benzyl group (Scheme 2) has been used to prepare DO3A terminal monomer **4** (in 94% overall yield) suitable for the conjugation with the peptide sequence. Purification of **4** by normal phase column chromatography (CH_2Cl_2–MeOH, 9 : 1) was found to be somewhat complicated by unexpected esterification of the glycine carboxylic group. Replacement of MeOH with MeCN resulted in the retention of the material on the column, even using higher proportions of MeCN. Although analytical samples of **4** have been obtained by careful chromatographic purification using an original solvent mixture, it was later found that purification of compound **4** was unnecessary as it can be subjected for the conjugation chemistry with the protected peptide attached to the resin without any significant yield loss.

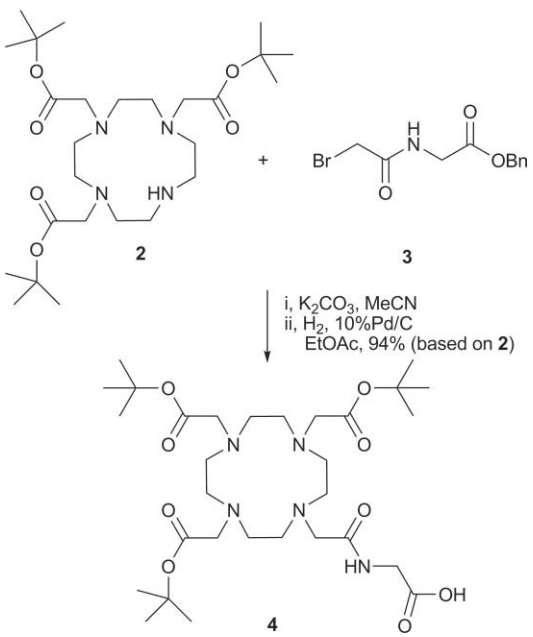

Scheme 2 Synthesis of DO3A terminal monomer **4**.

Conjugation of DO3A terminal monomer with the peptides, labeling with Oregon Green and metalation with $TmCl_3 \cdot 6H_2O$

Standard Fmoc peptide chemistry protocols[35] have been used to conjugate the DO3A terminal monomer **4** with fully protected (protecting groups are listed in the Experimental section) 22-mer peptides **5a** or **5b** attached to the resin (Scheme 3). Crude DO3A conjugated peptides **6a** or **6b** were cleaved off the resin (5% TES in wet TFA) and the residues obtained after drying were purified (see ESI†) by semi-preparative HPLC (details given in the Experimental section). Conjugate **6a** was obtained in 14%, whereas conjugate **6b** was obtained in 28% yield. Structures of both **6a** and **6b** were confirmed by mass spectrometry (high resolution ESI-TOF MS).

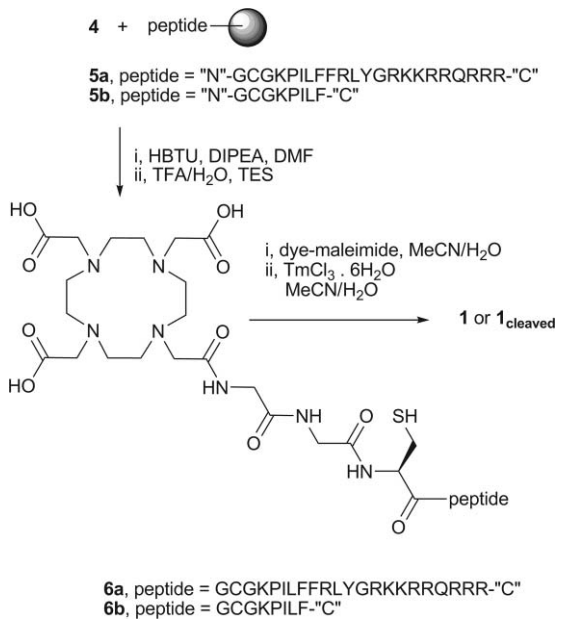

Scheme 3 Solid phase conjugation of DO3A terminal monomer **4** to fully protected peptides **5a** and **5b**, labeling with Oregon Green maleimide and subsequent metalation with $TmCl_3 \cdot 6H_2O$.

The resulting dual probe **1** was obtained in 78% yield, based on **6a**, and was purified by size exclusion chromatography. The Cat D-promoted cleavage product $\mathbf{1}_{cleaved}$ was obtained in 41% yield, based on **6b**. Absence of free Tm^{3+} in both **1** and $\mathbf{1}_{cleaved}$ was confirmed by xylenol orange test.[36] The structures of **1** (Fig. 1) and $\mathbf{1}_{cleaved}$ (Scheme 1) were confirmed by mass spectrometry (HR ESI-TOF, see ESI†). The protocol described above allows for the preparation of 10–20 mg of the dual probe **1** in one synthetic sequence.

Metabolism of the dual probe by cathepsin D

The enzymatic activity of Cat D toward probe **1** has been verified as depicted in Scheme 1 and described in the Experimental section. Cat D avidly digested probe **1**; thus, in order to observe the initial product of cleavage it was necessary to carefully determine the experimental conditions. It was also found necessary to use Pepstatin A, a well known inhibitor of aspartyl proteases,[37] to control the course of the reaction. By quenching the digestion after a short time, it was possible to observe both the unmetabolized probe **1** and a new signal that corresponded to the mass of metabolized probe $\mathbf{1}_{cleaved}$ simultaneously (Scheme 1, see ESI†, Fig. 4, Rt = 2.42 min). In order to confirm the molecular identity of the species that gave the signal at Rt = 2.42 min, we independently synthesized $\mathbf{1}_{cleaved}$ and analyzed it by the same UPLC-MS technique. Happily, it possessed the same retention time as the product observed in the mixture resulting from the digestion of probe **1** by Cat D. Longer incubation times did not increase the proportion of $\mathbf{1}_{cleaved}$ as this product itself is likely a substrate for further cleavage because it possesses lipophilic residues. However, we were unable to detect any other products of digestion.

Cell uptake studies

Cell uptake studies of probe **1**, possessing a cell penetrating peptide, were performed using SN56 cells because they possess neuronal properties which are relevant to our interest in Alzheimer's disease and because they were easily transfected. Cells were transfected with a DNA construct that induces high expression of human Cat D fused to mCherry (a red fluorescent protein). The cells were treated with 50 μM of **1** for 30 min at 37 °C and then the live cells were imaged using laser scanning confocal microscopy, and representative images are shown (Fig. 2). Panels B–D and F–H (Fig. 2) show laser scanning confocal epifluorescence images of Cat D (red) and **1** (green) with matching brightfield differential interference contrast (DIC) images (A and E). Cells that overexpressed Cat D–mCherry also took up and retained probe **1** (for example panel C) whereas cells that did not overexpress Cat D did not show intracellular accumulation of **1** (panel G). Cells were scored as containing or not containing contrast agent by an observer blinded to their transfection status. In 4 independent experiments, 17% (56/326) of cells took up and expressed the DNA construct encoding CatD–mRFP. Of these cells, 68.4 ± 4.9% (SEM) of transfected cells took up the contrast agent, showing bright green signal that was clearly intracellular (n = 56) whereas only 4.7 ± 1.3% (SEM) of untransfected cells (n = 270) took up the agent. Small amounts of the agent are sometimes seen outside of the cell bodies. Closer examination of cells overexpressing Cat D after incubation with probe **1** by fluorescence microscopy showed extensive punctuate distribution (data not shown).

MRI studies

MRI detection of fragment $\mathbf{1}_{cleaved}$ was demonstrated at 9.4 Tesla using the OPARACHEE method. To attribute a decrease in image intensity to chemical exchange, two images were acquired. The first image served as a control for altered T1 and T2 relaxation time constants induced by the paramagnetic lanthanide within the agent. The second image, acquired following application of an on-resonance WALTZ16 preparation pulse includes additional signal loss due to direct saturation and chemical exchange. The signal intensity difference between these images can be compared to the signal intensity difference observed in a sample without contrast agent to determine the on-resonance paramagnetic chemical exchange effect (OPARACHEE).

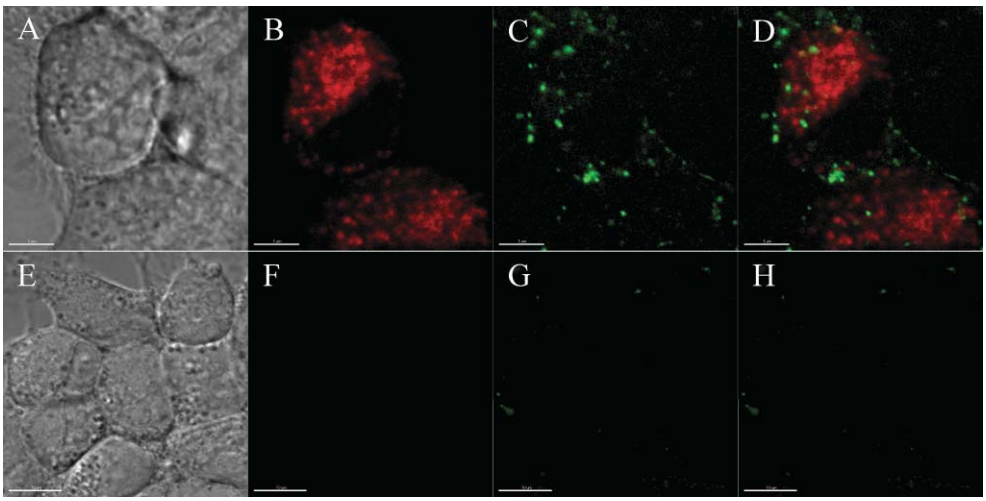

Fig. 2 SN56 cells overexpressing Cat D–mCherry internalize probe **1**. Images are of representative cells that expressed (A–D) or did not express (E–H) cathepsin-D–mCherry. Panels show brightfield microscopy (DIC) images (A and E), red fluorescent image channel (B and F), green fluorescent contrast agent image channel (C and G) and the green and red channels overlaid (D and H). Note that in typical cells transfected with CatD–mcherry, bright green fluorescence was observed clearly inside the cells. Small amounts of the agent were sometimes observed outside of cells (D–H). Scale bars are 5 μm (A–D) and 10 μm (E–H).

In addition to the $\mathbf{1}_{cleaved}$ molecular fragment, the conjugate **6b** containing neither Tm^{3+} nor the Oregon Green label was used as a control (control 2, Fig. 3), as well as a blank solvent mixture (8 : 2 H_2O–MeCN, control 1, Fig. 3). The relative decrease in signal intensity (% change) induced by the WALTZ-16 pulse was calculated for each sample and the resultant OPARACHEE contrast was determined (Fig. 3, panel C).

The average relative decrease in signal intensity (% change) for sample 1 was 41%, while it was only 19% and 17% for samples 2 and 3 respectively. Therefore, relative to the solvent mixture (control 1), $\mathbf{1}_{cleaved}$ produced a contrast of 24%, while **6b** (control 2) produced a contrast of 2%. The signal change observed in the control samples 1 and 2 was due to the direct saturation of the bulk water, while the change induced by the sample containing $\mathbf{1}_{cleaved}$ included the additional chemical exchange contrast induced by the lanthanide metal Tm^{3+}. These experiments confirm that the origin of the contrast is from the chelated metal and not due to the fluorophore or peptide fragment.

Conclusions

A dual (fluorescent microscopy/MRI) probe (**1**) designed to be metabolized by cathepsin D which contains a DOTA-derived metal chelator (metalated with Tm^{3+}), a fluorescent label (Oregon Green) and a peptide sequence (TAT peptide + Cat D cleavage site) is reported. Enzymatic degradation studies revealed that **1** was a substrate for Cat D, where mass spectrometry studies confirmed cleavage between the two phenylalanine residues. Fluorescence-based studies showed that the probe exhibited selective intracellular accumulation in cells that over-expressed cathepsin D. It is speculated that cleavage of the protease domain traps the probe within the cell. *In vitro* MRI contrast was realized using the OPARACHEE method. Further studies are aimed at exploiting the selective cellular accumulation and MR active group for molecular imaging applications.

Experimental

General experimental procedures

All reagents were commercially available. All solvents were HPLC grade and used as such, except for water which was deionized (18.2 MΩ cm^{-1}). Organic extracts were dried with Na_2SO_4 and solvents were removed under reduced pressure in a rotary evaporator. Flash column chromatography (FCC) was carried out using silica gel, mesh size 230–400 Å. Thin layer chromatography (TLC) was carried out on Al backed silica gel plates, compounds were visualized by UV light or I_2 vapors. Size exclusion chromatography was carried out on SEPHADEX G-25, 50–150 μm mesh resin (5 g, per 7.5 μmol of compound **1**). Ten fractions (3 mL each) were collected. Fractions containing the desired product were identified by fluorescence under UV illumination ($\lambda = 366$ nm). HPLC analysis and purification was carried out using a radial compression C18 300 Å column (particle size 15 μm; 8 × 100 mm) using a gradient elution. The mobile phases: Method A—90% H_2O–10% MeCN → 70% H_2O–30% MeCN over 30 min then 100% MeCN over 5 min; Method B—90% H_2O–10% MeCN → 40% H_2O–60% MeCN over 15 min then 100% MeCN over 5 min; Method C—90% H_2O–10% MeCN → 40% H_2O–60% MeCN over 20 min then 100% MeCN over 5 min; linear gradients, flow rates 3 mL min^{-1}. UPLC analysis was carried out using dual UV and mass (ESI-TOF) detection, with the separation performed on a C18 column (particle size 1.7 μm; 2.1 id × 50 mm). Mobile phase: Method D—100% H_2O → 25% H_2O–75% MeCN over 3 min, linear gradient, flow rate 0.25 mL min^{-1}. NMR spectra were recorded on 400 MHz spectrometer; for ^1H (400 MHz), δ values were referenced as follows $CDCl_3$ (7.26 ppm); for ^{13}C (100 MHz)

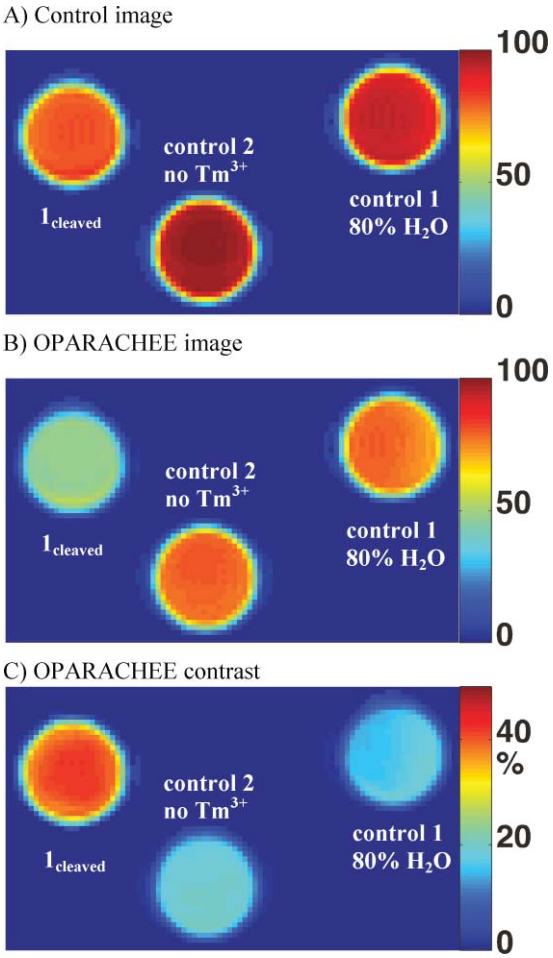

Fig. 3 PARACEST contrast agent MRI detection sensitivity. Samples vials are identified by labels, left to right: $\mathbf{1}_{cleaved}$; control 2: **6b**; control 1: 80% water–20% acetonitrile.

$CDCl_3$ (77.0 ppm). Mass spectra (MS) were obtained by electron spray ionization (ESI) time-of-flight (TOF) methods.

Preparation of *N*-bromoacetyl Gly-OBn (3)

A solution of bromoacetyl bromide (7.0 mL, 80 mmol) in CH_2Cl_2 (25 mL), was added dropwise over 1 h to a suspension of H-Gly-OBn·*p*-TsOH (25.3 g, 75 mmol) and DIPEA (26.5 mL, 150 mmol) in CH_2Cl_2 (200 mL) at –78 °C. The mixture was stirred for 12 h at room temperature and then washed with 1 M HCl (2 × 75 mL), saturated aqueous $NaHCO_3$ (75 mL), and brine (100 mL). The organic extract was dried, the solvent was evaporated and the residue was triturated with hexanes–Et_2O (9 : 1, 100 mL) and stored at 0 °C for 1 h. The solid was isolated by filtration to afford 14.4 g (66%) of the title compound. The spectral properties corresponded to those reported in the literature.[34]

Alkylation of DO3A *tert*-butyl ester (2) with *N*-bromoacetyl Gly-OBn (3) and reductive removal of the benzyl group

To a solution of DO3A-*tert*-butyl ester (**2**, 200 mg, 0.39 mmol) in MeCN (10 mL), were added K_2CO_3 (140 mg, 1.01 mmol) and *N*-bromoacetyl Gly-OBn (**3**, 111 mg, 0.39 mmol). The mixture was stirred for 18 h at 60 °C and subsequently concentrated to approximately 25% of its original volume and then was diluted with EtOAc (30 mL). The resulting mixture was washed with water (30 mL); the aqueous phase was extracted with EtOAc (20 mL). The combined organic extract was dried and the solvent was evaporated to leave a colorless oil of sufficient purity for the next reaction. This material was dissolved in EtOAc (6 mL) to which 10% Pd/C (140 mg) was added and the mixture was vigorously stirred under an atmosphere of H_2 at room temperature for 18 h. The catalyst was filtered off using a CELITE pad, the filter was washed with MeOH and the filtrate was concentrated to afford 230 mg (94%, based on **3**) of DO3A terminal monomer **4**. Analytical samples of **4** were obtained by FCC on 20 g SiO_2 (CH_2Cl_2–MeOH, 9 : 1). ^{1}H NMR δ 6.99 (m, D_2O exch., 1H); 3.75 (br s, 2H); 3.36 (br s, 4H); 2.89-2.15 (br m, 20 H); 1.44 (m, 27H); ^{13}C NMR ($CDCl_3$) δ 172.5, 172.3, 170.3, 169.3, 82.2, 82.0, 56.4, 55.7, 55.6, 44.3, 28.0, 27.9. HRMS (ESI) *m*/*z*: found 630.4073 $[M+H]^+$ (630.4078 calcd for $C_{30}H_{56}N_5O_9$).

Conjugation of DO3A terminal monomer 4 with protected peptides 5a and 5b

In a separate peptide synthesis vessels, resins containing the protected (R-Pbf, C-Trt, Q-Trt, K-Boc, Y-*t*Bu, '*N*' terminal-Fmoc) peptides **5a** (*N*-GCG-KPI-LFF-RLY-GRK-KRR-QRR-R-*C*, 2.66×10^{-5} mol, 100 mg of the resin) or **5b** (*N*-GCG-KPI-LF-*C*, 3.00×10^{-5} mol, 50 mg of the resin) were treated with 20% piperidine in DMF (2 mL, repeated twice) for 5 min. The resins were consecutively washed with dry DMF and CH_2Cl_2 (*ca.* 2 × 10 mL each, repeated twice). In a separate vials DIPEA (32 µL, 1.85×10^{-4} mol, to conjugate with **5a**; 37 µL, 2.10×10^{-4} mol, to conjugate with **5b**) and HBTU (32 mg, 8.28×10^{-5} mol, to conjugate with **5a**; 36 mg, 9.45×10^{-5} mol, to conjugate with **5b**) were added to a cooled (0 °C) solutions of DO3A terminal monomer **4** (60 mg, 9.31×10^{-5} mol, to conjugate with **5a**; 66 mg, 1.05×10^{-4} mol, to conjugate with **5b**) in DMF (700 µL). The resulting mixtures were added (after 10 min at 0 °C) to the washed resins in the separated peptide vessels followed by agitation for 1.5 h at rt. The resins were washed as described above and were treated with cleavage cocktail (5 mL, for 2 h at rt) prepared by dissolving water (300 µL) and TES (200 µL) in TFA (10 mL). The obtained TFA solutions were concentrated to *ca.* 10% of their original volumes, were cooled to 0 °C, cold (–20 °C) Et_2O (20 mL) was added and the mixtures were set aside for 1 h at –20 °C. The resulting mixtures were centrifuged (3 min at 1000 rpm); the supernatants were decanted and discarded and the recovered pellets were dissolved in water (3 mL). The resulting solutions were lyophilized to afford the crude peptide conjugates **6a** (46 mg) or **6b** (28 mg). These materials were purified by semi-preparative HPLC as described in the General experimental procedures. Conjugate **6a** (Method A, 12.1 mg, 14% based on **4**); colorless solid; HPLC: t_R 25.1 min; HRMS (ESI) *m*/*z*: found 3235.8900 $[M+H]^+$ (3235.8578 calcd for $C_{142}H_{241}N_{52}O_{33}S$). Conjugate **6b** (Method B, 10.8 mg, 28% based on **4**); colorless solid; HPLC: t_R 8.3 min; HRMS (ESI) *m*/*z*: found 1277.6594 $[M+H]^+$ (1277.6564 calcd for $C_{57}H_{93}N_{14}O_{17}S$).

Labeling of conjugates 6a and 6b with Oregon Green and metalation with $TmCl_3 \cdot 6H_2O$

Separate solutions of conjugates **6a** (24.3 mg, 7.50×10^{-6} mol) or **6b** (5.4 mg, 4.20×10^{-6} mol) in water (**6a**, 2 mL; **6b**, 600 µL)

were added to separate solutions of Oregon Green maleimide (3.5 mg, 7.50×10^{-6} mol, to conjugate with **6a**; 1.9 mg, 4.20×10^{-6} mol, to conjugate with **6b**) in MeCN (600 μL). The mixtures were stirred for 48 h at rt in the dark, after which time they were frozen and lyophilized to afford an orange solid residues. These were dissolved in a mixtures of water (1.5 mL) and MeCN (500 μL), to conjugate with **6a** or water (600 μL) and MeCN (600 μL), to conjugate with **6b** and separate solutions of $TmCl_3 \cdot 6H_2O$ (0.1 M, 225 μL, 2.25×10^{-5} mol to conjugate with **6a**; 0.1 M, 126 μL, 1.26×10^{-5} mol to conjugate with **6b**) were added. The mixtures were stirred for 48 h at rt in the dark and were purified as follows. The mixture containing the dual probe **1** was subjected to size exclusion chromatography as described in General experimental procedures. Fractions containing the product were combined and were lyophilized to afford 22.5 mg (78%) of the dual probe **1** as an orange solid; HRMS (ESI) *m/z*: found 3863.7924 $[M - 2H]^+$ (3863.8110 calcd for $C_{166}H_{249}F_2N_{53}O_{40}STm$). The mixture containing the Cat D cleavage product $\mathbf{1}_{cleaved}$ was subjected to semi-preparative HPLC as described in the General experimental procedures. Conjugate **6b** (Method C, 3.3 mg, 41%); orange solid; HPLC: t_R 14.7 min; HRMS (ESI) *m/z*: found 1906.6208 $[M+H]^+$ (1906.6175 calcd for $C_{81}H_{101}F_2N_{15}O_{24}STm$). The absence of unchelated Tm^{3+} in the resulting conjugates **1** and $\mathbf{1}_{cleaved}$ was confirmed as described previously.[36]

Cell culture

SN56 cells were a gift from Dr Jane Rylett (The University of Western Ontario). SN56 cells were derived from septum neurons (Septal neurons X neuroblastoma N18TG2)[38] and present a number of neuronal features including expression of synaptic vesicle proteins[39] and neuronal type calcium channels. These features are increased by differentiation.[40,41] Cells were maintained in Dulbecco's modified Eagle's medium supplemented with 5% fetal bovine serum and 1% penicillin/streptomycin. Cell differentiation was performed with the addition of 1 mM dibutyryl-cyclic AMP in the same medium without fetal bovine serum for 24 h. Transient transfections were performed using Lipofectamine 2000 according to the manufacturer's instructions.

Constructs

An mCherry (a red monomeric fluorescent protein) cDNA was a gift from Dr Roger Tsien (University of California, San Diego). mCherry was amplified using PCR using primers that appended 5′ BamH1 and 3′ Not1 restriction sites and used to replace EGFP in the pEGFP-N1 expression vector plasmid. A cDNA encoding cat D was amplified using primers that delete the terminal stop codon and append 5′Xho1 and 3′HindIII restriction sites and cloned into the mCherry expression vector. This plasmid drives high level expression of the inserted cat D-mCherry fusion protein immediate early promoter of CMV.

Cellular uptake and confocal laser scanning microscopy

Cells were grown in 35 mm glass-bottomed culture dishes for confocal studies. Cells were incubated at 37 °C for 30 min with compound **1** added to media (50 μM). After incubation, the media and contrast agent were removed and replaced with Hanks buffered saline solution. Confocal microscopy was performed on a laser-scanning confocal microscope using a 63 × 1.4 numerical aperture oil immersion lens. The contrast agent was visualized using a 488 nm excitation laser and a 500–530 nm emission filter set. Red fluorescence from the Cat D–mCherry fusion protein as imaged using a 543 nm excitation laser and LP 560 filter set.

Cathepsin D enzymatic cleavage of 1

Cleavage of **1** (40 pmol) was performed with Cat D (0.01 units) from bovine spleen in 100 μl of 150 mM NaCl with 20 mM citrate-phosphate buffer at a pH of 4.5. Cleavage proceeded at 37 °C for 5 min and the reaction was stopped by the addition of the inhibitor pepstatin A (2.5 μg). The resulting mixtures were analyzed by UPLC-MS(ESI-TOF) operating under conditions described earlier, *vide supra*. The identity of the initial cleavage product, $\mathbf{1}_{cleaved}$, was confirmed by independent synthesis. The synthetic $\mathbf{1}_{cleaved}$ possessed the same retention time as the product of initial cleavage of **1** by Cat D.

MRI studies with $\mathbf{1}_{cleaved}$

Detection of $\mathbf{1}_{cleaved}$ by MRI was verified using a 9.4 Tesla, 31 cm diameter bore Varian (Palo Alto, CA) small animal MRI scanner. Three samples were prepared for imaging. Sample 1 contained 3 mM $\mathbf{1}_{cleaved}$ dissolved in 80% water–20% acetonitrile. Sample 2 contained 3 mM of an unmetallated version of $\mathbf{1}_{cleaved}$ without the Oregon Green label (conjugate **6b**) dissolved in 80% water–20% acetonitrile. Sample 3 contained only 80% water–20% acetonitrile. All three samples were placed in the MRI scanner (21 °C) and two single slice images were acquired using a fast low angle shot (FLASH) pulse sequence (TE/TR = 2.5/5.3 ms, 25.6 mm × 25.6 mm field of view, 128 × 128 matrix, 3 mm thick, 5 s pre-delay). The first image was considered the control image. Preceding the second image, a WALTZ-16 (480 ms, 6 μT) preparation pulse was centered on the bulk water frequency to generate OPARACHEE contrast. The percent change in signal intensity within each sample (% change) was calculated on a pixel-by-pixel basis by taking the difference between the signal intensity in the first FLASH control image (I_0) and the FLASH image acquired following the WALTZ-16 preparation pulse (I_s) and normalizing to the average signal intensity within each sample in the control FLASH image.

Acknowledgements

The authors gratefully acknowledge funding received from the Ontario Institute for Cancer Research (OICR), Canada to support this work. Gifts of materials are gratefully acknowledged from Professors Roger Tsein (University of California, San Diego) and Jane Rylett (The University of Western Ontario).

Notes and references

1 H. Rochefort, *Breast Cancer Res. Treat.*, 1990, **16**, 3.
2 A. Losch, M. Schindl, P. Kohlberger, J. Lahodny, G. Breitenecker, R. Horvat and P. Birner, *Gynecol. Oncol.*, 2004, **92**, 545.
3 I. Dvalishvili, L. Charkviani, T. Charkviani, G. Turashvili and G. Burkadze, *Georgian Med. News*, 2005, 27.
4 S. Konno, J. P. Cherry, J. A. Mordente, J. R. Chapman, M. S. Choudhury, C. Mallouh and H. Tazaki, *World J. Urol.*, 2001, **19**, 234.
5 H. Rochefort, F. Capony and M. Garcia, *Cancer Metastasis Rev.*, 1990, **9**, 321.

6 G. Leto, F. M. Tumminello, M. Crescimanno, C. Flandina and N. Gebbia, *Clin. Exp. Metastasis*, 2004, **21**, 91.
7 E. Liaudet-Coopman, M. Beaujouin, D. Derocq, M. Garcia, M. Glondu-Lassis, V. Laurent-Matha, C. Prebois, H. Rochefort and F. Vignon, *Cancer Lett.*, 2006, **237**, 167.
8 P. Benes, V. Vetvicka and M. Fusek, *Crit. Rev. Oncol. Hematol.*, 2008, **68**, 12.
9 A. M. Cataldo, J. D. Barnett, S. A. Berman, J. Li, S. Quarless, S. Bursztajn, C. Lippa and R. A. Nixon, *Neuron*, 1995, **14**, 671.
10 A. M. Cataldo and R. A. Nixon, *Proc. Natl. Acad. Sci. U. S. A.*, 1990, **87**, 3861.
11 A. L. Schwagerl, P. S. Mohan, A. M. Cataldo, J. P. Vonsattel, N. W. Kowall and R. A. Nixon, *J. Neurochem.*, 1995, **64**, 443.
12 R. E. Kohnken, U. S. Ladror, G. T. Wang, T. F. Holzman, B. E. Miller and G. A. Krafft, *Exp. Neurol.*, 1995, **133**, 105.
13 N. Chevallier, J. Vizzavona, P. Marambaud, C. P. Baur, M. Spillantini, P. Fulcrand, J. Martinez, M. Goedert, J. P. Vincent and F. Checler, *Brain Res.*, 1997, **750**, 11.
14 For the recent review on the diagnostics of Alzheimer's disease see: P. Lewczuk and J. Wiltfang, *Proteomics*, 2008, **8**, 1292.
15 For the seminal paper introducing this concept see: K. M. Ward, A. H. Aletras and R. S. Balaban, *J. Magn. Reson.*, 2000, **143**, 79.
16 For the recent reviews on PARACEST MRI CAs see: (*a*) M. Woods, D. E. Woessner and A. D. Sherry, *Chem. Soc. Rev.*, 2006, **35**, 500; (*b*) A. D. Sherry and M. Woods, *Annu. Rev. Biomed. Eng.*, 2008, **10**, 391.
17 R. S. Zhang, M. Merrit, D. E. Woessner, R. Lenkinski and A. D. Sherry, *Acc. Chem. Res.*, 2003, **36**, 783.
18 T. Chauvin, P. Durand, M. Bernier, H. Meudal, B. T. Doan, F. Noury, B. Badet, J. C. Beloeil and É. Tóth, *Angew. Chem., Int. Ed.*, 2008, **47**, 4370.
19 (*a*) B. Yoo and M. D. Pagel, *J. Am. Chem. Soc.*, 2006, **128**, 14032; (*b*) B. Yoo, M. S. Raam, R. M. Rosenblum and M. D. Pagel, *Contrast Media Mol. Imaging*, 2007, **2**, 189.
20 B. Yoo, V. R. Sheth and M. D. Pagel, *Tetrahedron Lett.*, 2009, **50**, 4459.
21 F. Wojciechowski, M. Suchý, A. X. Li, H. A. Azab, R. Bartha and R. H. E. Hudson, *Bioconjugate Chem.*, 2007, **18**, 1625.
22 A. X. Li, F. Wojciechowski, M. Suchý, C. K. Jones, R. H. E. Hudson, R. Menon and R. Bartha, *Magn. Reson. Med.*, 2008, **59**, 374.
23 M. Suchý, A. X. Li, R. Bartha and R. H. E. Hudson, *Bioorg. Med. Chem.*, 2008, **16**, 6156.
24 M. Suchý, A. X. Li, R. Bartha and R. H. E. Hudson, *Org. Biomol. Chem.*, 2008, **6**, 3588.
25 T. Jiang, E. S. Olson, Q. T. Nguyen, M. Roy, P. A. Jennings and R. Y. Tsien, *Proc. Natl. Acad. Sci. U. S. A.*, 2004, **101**, 17867.
26 For the recent review on the use of cell penetrating peptides in drug delivery see: K. M. Stewart, K. L. Horton and S. O. Kelly, *Org. Biomol. Chem.*, 2008, **6**, 2242.
27 MEROPS database http://merops.sanger.ac.uk. The core cleavage sequence (ILFFRL) registered three hits: Cathepsin E, Pepsin F and Cad3 peptidase. The biodistribution of Cat D is much different that Cat E (ref. 31), especially in the brain which is one of the primary targets of interest for this work since Cat D is associated with Alzheimer's disease. Pepsin F is a digestive protease and is of little consequence for contrast agents that are administered intravenously and Cad3 is a digestive protease from *Musca domestica* (housefly).
28 E. Vinogradov, H. He, A. Lubag, J. A. Balschi, A. D. Sherry and R. E. Lenkinski, *Magn. Reson. Med.*, 2007, **58**, 650.
29 E. Vinogradov, S. Zhang, A. Lubag, J. A. Balschi, A. D. Sherry and R. E. Lenkinski, *J. Magn. Reson.*, 2005, **176**, 54.
30 Oregon Green absorbs at 491 nm and emits at 515 nm.
31 Y. Yasuda, T. Kageyama, A. Akamine, M. Shibata, E. Kominami, Y. Uchiyama and K. Yamamoto, *J. Biochem.*, 1999, **125**, 1137.
32 J. Higaki, R. Catalano, A. W. Guzzetta, D. Quon, J. F. Navé, C. Tarnus, H. D'Orchymont and B. Cordell, *J. Biol. Chem.*, 1996, **271**, 31885.
33 For the recent review on the functionalization of cyclen and its simple derivatives see: M. Suchý and R. H. E. Hudson, *Eur. J. Org. Chem.*, 2008, 4847.
34 Synthesis of compound **3** has been recently described, see: R. Scheffelaar, R. A. K. Nijenhuis, M. Paravidino, M. Lutz, A. L. Spek, A. W. Ehlers, F. J. J. de Kanter, M. B. Groen, R. V. A. Orru and E. Ruijter, *J. Org. Chem.*, 2009, **74**, 660.
35 For a recent review on DOTA peptide conjugates see: L. M. De León-Rodríguez and Z. Kovács, *Bioconjugate Chem.*, 2008, **19**, 391.
36 A. Barge, G. Cravotto, E. Gianolio and F. Fedeli, *Contrast Media Mol. Imaging*, 2006, **1**, 184.
37 J. Marciniszyn, J. A. Hartsuck and J. Tang, J., *J. Biol. Chem.*, 1976, **251**, 7088.
38 D. N. Hammond, H. J. Lee, J. H. Tonsgard and B. H. Wainer, *Brain Res.*, 1990, **512**, 190.
39 J. Barbosa, A. R. Massensini, M. S. Santos, S. I. Meireles, R. S. Gomez, M. V. Gomez, M. A. Romano-Silva, V. F. Prado and M. A. M. Prado, *J. Neurochem.*, 1999, **73**, 1881.
40 C. Kushmerick, M. A. Romano-Silva, M. V. Gomez and M. A. M. Prado, *Brain Res.*, 2001, **916**, 199.
41 J. K. Blusztajn, A. Venturini, D. A. Jackson, H. J. Lee and B. H. Wainer, *J. Neurosci.*, 1992, **12**, 793.

